

Iodine Treatment of Lignin–Cellulose Acetate Electrospun Fibers: Enhancement of Green Fiber Carbonization

Makoto Schreiber,^{†,‡} Singaravelu Vivekanandhan,^{†,§} Amar Kumar Mohanty,^{†,§} and Manjusri Misra^{*,†,§}

[†]Bioproducts Discovery and Development Centre, Department of Plant Agriculture, Crop Science Building, University of Guelph, 50 Stone Road East, Guelph N1G 2W1, Ontario, Canada

[‡]Department of Physics, University of Guelph, 50 Stone Road East, Guelph N1G 2W1, Ontario, Canada

[§]School of Engineering, Thornborough Building, 50 Stone Road East, University of Guelph, Guelph N1G 2W1, Ontario, Canada

ABSTRACT: Pure biopolymer-based electrospun precursor carbon fibers are fabricated using an abundant and inexpensive biopolymer lignin blended with renewable resource-based cellulose acetate (CA). Iodine treatment on the fabricated green fiber was successfully performed in order to enhance the carbonization process as well as the retention of fiber morphology. The absorption mechanism of iodine by lignin and cellulose acetate and their derived electrospun green fibers has been investigated by means of thermal behavior and morphological retention. It was found that iodine treatment plays a vital role in altering the graphitization behavior as well as morphology retention during the carbonization process. With the help of iodine treatment, the green precursor fibers were successfully converted into thin carbon fibers, and scanning electron microscopy analysis confirmed the retention of fibrous structures with diameters around 250 nm. Raman spectroscopy revealed that although the overall level of graphitization was lower compared to polyacrylonitrile-based fibers, the graphitic crystallite size was larger in the produced carbon fibers. The produced pure biopolymer fibers and iodine treatments show promise for the production of green and cost-reduced carbon fibers.

KEYWORDS: Lignin, Carbon fiber, Electrospinning, Raman spectroscopy, Iodine



INTRODUCTION

Carbon fibers (CFs) are industrially important materials due to their excellent properties such as high strength, being lightweight, electrical/thermal conductivity, and other functional properties.^{1,2} Recently, there has been an increased demand for cheaper and more available CFs, especially carbon nanofibers. A recent method of producing these submicron diameter CFs is through electrospinning,^{3–6} which produces CFs in a manner close to that of traditionally produced CFs through spinning, oxidizing, and carbonizing. In this method, a polymer is dissolved in an appropriate solvent, which through electrostatic forces, is pulled into a long continuous fiber. The electrospun fibers are then thermally stabilized by heating slowly to a temperature around 300 °C; which causes cross links to form in the fiber structure through oxidative reactions that increase the thermal stability of the fiber. The stabilized fibers are then carbonized by heating to high temperatures (over 600 °C and as high as 3000 °C) in an inert atmosphere to remove the noncarbon elements and rearrange the carbon bonds.⁷ Electrospinning is utilized as it is a very simple technology that can easily produce continuous submicron diameter fibers from a wide variety of precursor materials.⁸ The shear forces exerted on the electrospinning jet can also induce some molecular orientation within the fibers⁹ that can improve graphitization in the CFs.^{10,11}

Although it is possible to produce submicron diameter CFs, an issue still remains with the raw precursor materials required. Currently, 90% of the commercially available CFs are produced from polyacrylonitrile (PAN),¹² with the remaining being from petroleum pitch. Both of these precursors are reliant on petroleum resources and are costly, especially PAN. Thus, both the availability and cost of the precursors hinder the production of CFs, which is below 13,000 tons/year.¹³ Recently, a few researchers have been looking at lignin as a potential precursor material for CFs^{13–17} as it is a highly abundant biomaterial with a high carbon content produced as a coproduct of the pulp and paper and cellulosic ethanol industries. From the pulp and paper industry alone, there is an estimated annual production of 70 million tons,¹⁸ with little application besides being used as a low quality fuel.¹² In most cases, especially for electrospun fibers, it is required to blend the lignin with another polymer in order to successfully spin fibers;^{19–21} PAN and poly(ethylene oxide) are commonly used. Although pure lignin carbon fibers have been previously spun using conventional processes, their properties have not been up to par with conventional CFs in terms of mechanical properties.¹² However, it can be used to substitute some of the PAN in a blend without reduction of the

Received: July 25, 2014

Revised: October 27, 2014

Published: November 6, 2014

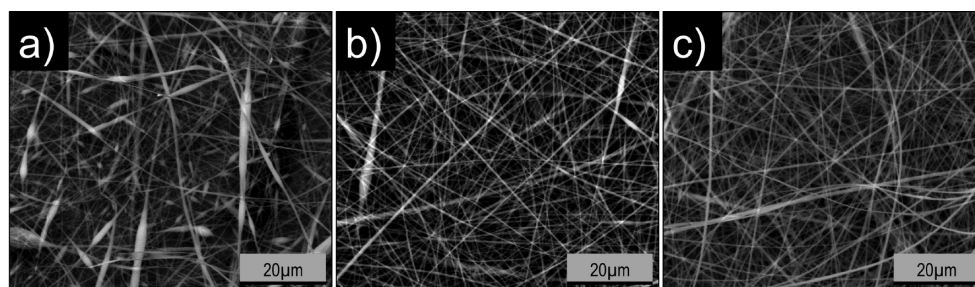


Figure 1. SEM micrographs of the electrospun CA fibers from solution concentrations of (a) 15, (b) 18, and (c) 20 wt %.

mechanical properties.¹² Recently, Choi et al. have demonstrated that high lignin content CFs have the potential to be used as lithium-ion battery anodes due to the high cycling performance they measured in their experiments.¹⁹ Chatterjee et al. have also shown that the structural characteristics of lignin-based carbon fibers include graphitic domains in an amorphous matrix, which help prevent exfoliation of the graphite due to the solid electrolyte interface that forms in a Li-ion battery.²² Thus, it is also desirable to fabricate lignin-based CFs for electrical applications. In this case, as the mechanical properties are not as crucial, it would be desirable to produce lignin-based CFs that do not utilize any synthetic polymers; such as a fully biopolymer-derived carbon fiber. These fibers would have the added benefit of a lower cost due to the lower polymer costs (compared to PAN) as well as solvent costs and much lower solvent toxicities (compared to the dimethylformamide commonly used to dissolve PAN). Depending on the type of lignin used, different blend polymers are required as the different lignins can have quite different properties such as charge and solubility. In a previous work, the authors electrospun precursor fibers from an anionic water-soluble lignin with chitosan.²³ As the lignin used in this work is an organosolv lignin rather than a water-soluble lignin, a different blend polymer was required.

Another challenging aspect of the conversion of precursor fibers into CFs is the retention of the fibrous morphology during the carbonization process. During the heating process, if the temperature increases above the glass transition temperature (T_g) of the precursor fibers, the fibers can soften and fuse together. Thus, the material is usually heated slowly in the thermal stabilization stage to allow oxidative reactions to increase the T_g of the material above that of the heating temperature. In some cases, this process is not effective on its own but can be enhanced by pretreating the fibers. This is especially important for fine submicron diameter fibers. Iodine has been investigated as a treatment to enhance the thermal treatment process of various materials during the carbonization process such as pitch and silk fibers.^{24–29} Iodine is known to form charge transfer complexes (CTCs) with electron-rich molecules such as those with lone pairs and aromatic rings in the form of polyiodides.^{29,30} Bromine is another halogen that has been studied for enhancement of the carbonization process and has been compared with iodine.^{26,31} It was found that bromination is nonselective and localized, while iodination was selective to aromatics and nonlocalized, iodinating throughout the material. Thus, iodine is better suited to evenly treat a material for carbonization. The thermal stabilization process is enhanced with iodine treatments as, through the heating process, the iodine and absorbate forming the CTC react to form HI, which leaves behind a free radical.²⁵ Thus, this

dehydrogenation promotes cross-linking reactions within the iodine treated materials, improving and speeding up the thermostabilization process. To the authors' knowledge, iodine treatments have not yet been investigated toward lignin. Thus, in this paper, we investigate the electrospinning of lignin blended with cellulose acetate (CA) dissolved in a blend of acetone and N,N-dimethylacetamide (DMAc) to produce green precursor fibers. The effects of iodination on lignin and the lignin-based electrospun fibers are then investigated in order to produce green CFs.

EXPERIMENTAL SECTION

Materials. Hardwood organosolv lignin (LL) powder was graciously provided by Lignol Innovations, Ltd., Burnaby, BC, Canada. Cellulose acetate, CA (average $M_n \sim 30,000$ by GPC, 39.8 wt % acetyl) and acetone were purchased from Sigma-Aldrich. DMAc was purchased from Fisher Scientific. Iodine crystals were purchased from The Nichols Chemical Company, Limited. All materials were used as received.

Electrospinning of Fibers. Pure CA solutions of 15, 18, and 20 wt % (g/mL) were prepared in a 2:1 mixture of acetone and DMAc. The electrospinning solution blends were prepared by mixing LL and CA into the 2:1 acetone:DMAc. A constant total polymer concentration of 30 wt % was maintained across all solutions. Solutions with LL:CA ratios of 1:1, 2:1, 3:1, 4:1, and 5:1 were prepared. The solutions were then electrospun in a NANON-01A electrospinning setup (MECC Co., Ltd. Japan) using a working distance of 22.5 cm, 24 gauge capillary, 0.7 mL/h feed rate, and 16–18 kV applied voltage onto a stationary plate collector.

Iodine Treatment of Lignin, Cellulose Acetate, and Electrospun Fibers. The as-received LL and CA powders were placed into ceramic boats that were then placed into sealed glass jars containing iodine crystals. The electrospun fibers were separated from the plate collector, wrapped around a rectangular metal frame, placed into a ceramic boat, and then placed into the jars with iodine. The iodine jars were placed into a 100 °C oven to vaporize the iodine for set time periods. After removal of the jars from the oven, they were allowed to cool (so all the remaining iodine vapor recrystallized) before the samples were removed.

Thermostabilization and Carbonization. Iodine-treated and nontreated samples were thermally treated to convert them into carbonaceous materials. The thermal treatments of the samples were carried out in a carbolite 1200 °C G-range tube furnace. Thermostabilization was performed by heating the samples at 2 °C/min to 300 °C in an air atmosphere and holding for 2h. Carbonization was performed by heating samples at 2 °C/min to 600, 800, 1000, or 1200 °C and holding for 1 h.

Characterization. The samples were characterized for their morphology, chemical composition, and thermal stability. The sample morphology was investigated using an FEI-Inspect S50 scanning electron microscope (SEM). The images were analyzed using the ImageJ software, and fiber diameters were calculated from at least 40 measurements. The chemical composition of the samples were analyzed using an Oxford Instruments X-Max20 energy dispersive X-ray spectrometer (EDS), Thermo Scientific Nicolet 6700 Fourier

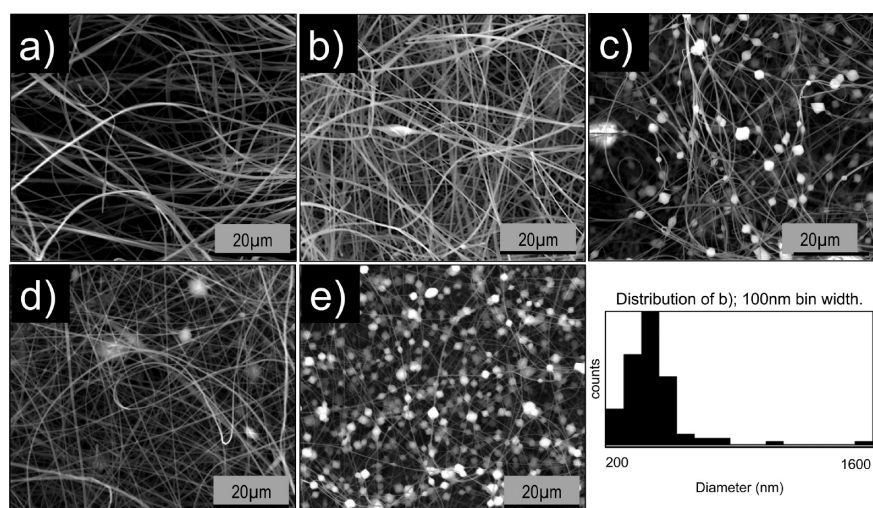


Figure 2. SEM micrographs of the electrospun blend fibers with LL:CA ratios of (a) 1:1, (b) 2:1, (c) 3:1, (d) 4:1, and (e) 5:1. The histogram shows an example diameter distribution as measured for the 2:1 LL:CA fibers.

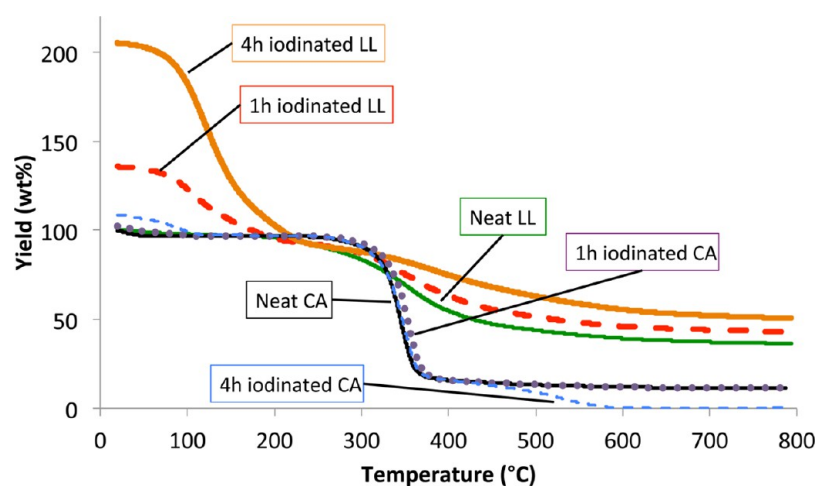


Figure 3. TGA thermograms of neat LL and CA powders as well as LL and CA powders iodine treated for the indicated times. The yields are normalized to the mass of the samples prior to iodine treatments.

transform infrared (FTIR) spectrometer with a GladiATR single reflection ATR accessory (operated between 400 and 4000 cm^{-1} with a 4 cm^{-1} resolution averaged over 40 scans), and Renishaw Raman spectrometer operated using a 785 nm near-infrared laser (1100–1900 cm^{-1} with a 0.8 cm^{-1} resolution averaged over 3 scans). The Raman peaks were fitted using Lorentzian curves and baseline corrected with a cubic function with the Igor Pro software Multipeak Fit 2 tool. The thermal stabilities of the samples were measured with a TA Instruments Q500 thermogravimetric analyzer (TGA) heating at 10 $^{\circ}\text{C}/\text{min}$ to 800 $^{\circ}\text{C}$ in an N_2 atmosphere.

RESULTS AND DISCUSSIONS

Electrospun Fibers. The 20 and 18 wt % CA solutions could be successfully electrospun into fiber mats that could be easily removed from the plate collector intact, while the 15 wt % CA solution did not form such fibers; the mat tearing upon removal. From the SEM images (Figure 1), it is clear that the 15 wt % CA fibers were much weaker because they were highly beaded with elongated bead defects that severely weakened the fibers compared to the defect-free 18 and 20 wt % CA fibers. Thus, the electrospinning performance of the CA solutions is highly dependent on the concentration. The 1:1, 2:1, 3:1, and 4:1 ratio LL:CA solutions formed fiber mats successfully, which

could be extracted from the collector. However, the 5:1 solution failed to form a fiber mat that could be removed from the plate collector. SEM micrographs of the fibers are shown in Figure 2. As shown, the 5:1 fibers were almost completely beaded and like the 15 wt % CA fibers were very weak. Thus, there was likely not enough CA in the blend to facilitate the electrospinning process. Of the other LL:CA fibers, the 1:1 ratio had the least defects and the 3:1 ratio had the most. The 2:1 and 4:1 ratios appeared to have similarly low levels of beading. The higher incidence of beading in the 3:1 ratio fibers could be due to a low point in the viscosity profile as previously explored.³² The fiber diameters did not differ significantly between the fibers; all of them being close to 450 nm with about 100 nm in standard deviation. A representative histogram of the fiber diameter distribution is also shown in Figure 2 showing that a roughly normal distribution is produced, with a few outlying larger diameters. Thus, the LL:CA ratio plays a key role in the formation of the fiber mats with the desired morphological features

Although LL could not be electrospun by itself and pure CA fibers from solutions of 15 wt % and below could not be electrospun, all the blend solutions contained 15 wt % CA or

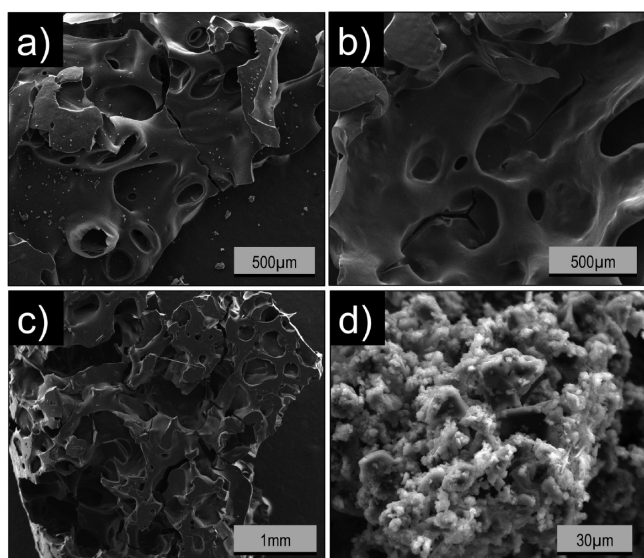


Figure 4. SEM micrographs of (a) neat CA, (b) 5 h iodinated CA, (c) neat LL, and (d) 5 h iodinated LL after being thermostabilized at 300 °C for 2 h in air then carbonized at 600 °C for 1 h in N₂.

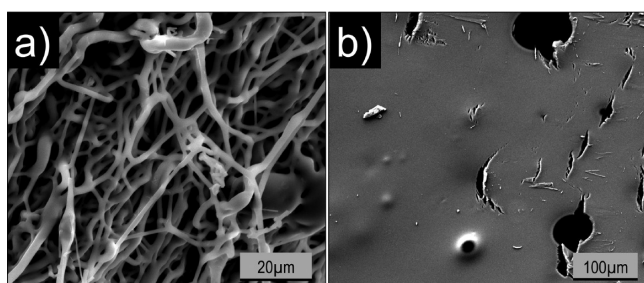


Figure 5. SEM micrographs of (a) 3:1 LL:CA fibers just before collapse of the fibrous structure from the iodine treatment and (b) 1:1 LL:CA fibers after collapsing from 1 h iodine treatment.

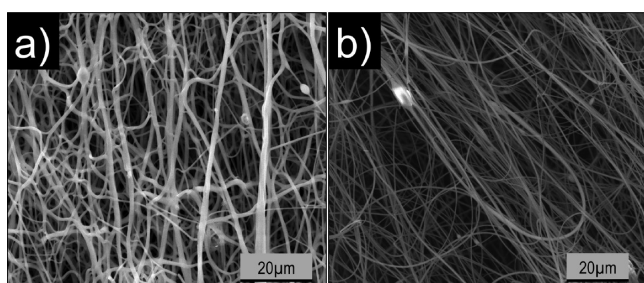


Figure 6. SEM micrographs of the 2:1 ratio LL:CA fibers after being thermostabilized at 300 °C for 2 h in air: (a) untreated and (b) 20 min iodinated LL:CA fibers.

less, thus showing that there was an excellent interaction between LL and CA. The interaction was likely due, in part, to hydrogen bonding between the hydroxy groups on LL and the acetyl groups on CA. Furthermore, previous work by Glasser and Davé^{33,34} on lignin blended with cellulose derivatives has shown that with the addition of lignin to the cellulose derivatives, a mesophasic nanoscale liquid crystalline architecture is formed due to the lignin disrupting the crystalline and noncrystalline order of the cellulosic phase. Although the lignin content in this work is much higher than in the work by Glasser and Davé, a similar two-phase structure may be formed in the

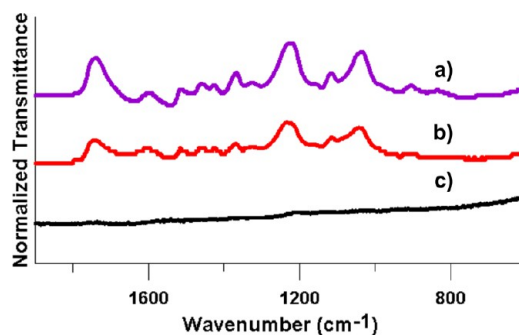


Figure 7. FTIR spectra of 2:1 ratio LL:CA fibers normalized to the 1600 cm⁻¹ lignin aromatic peak: (a) as-spun fibers, (b) fibers iodinated for 20 min and thermostabilized at 300 °C in air for 2 h, and (c) fibers iodinated, thermostabilized, and then carbonized at 800 °C for 1 h.

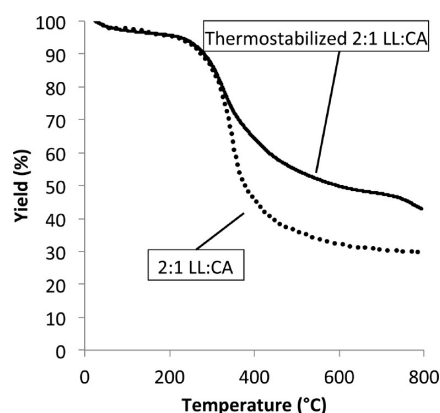


Figure 8. TGA thermograms of 2:1 ratio LL:CA fibers as-spun and after being iodinated for 20 min and thermostabilized at 300 °C for 2 h.

LL:CA fibers and will be further investigated in future works. The constant 30 wt % total polymer concentration used for all the LL:CA blend fibers was also a higher concentration than pure CA could be spun at, which is beneficial for reducing solvent costs. This is possible due to the low intrinsic viscosity of lignin,^{34,35} which allows the solution to flow easier. Some higher total polymer concentrations were attempted but resulted in the electrospinning droplet solidifying at the needle almost immediately. Thus, these two biopolymers were found to interact very well to allow the fabrication of a pure biobased precursor carbon fiber.

Effects of Iodine Treatments on neat LL and CA. The iodine absorption capacity of the neat LL and CA powders were investigated through iodinations at 1 h intervals from 1 to 7 h and one at 24 h. LL-absorbed iodine readily as expected from its highly aromatic structure, changing from a light brown to black after treatment. After 1 h of iodination, the weight of LL increased by about 35 wt %. After 4 h, an over 100 wt % gain was measured, and at 24 h, LL gained about 154 wt %. Thus, in the first few hours, there is a rapid uptake of iodine into LL that slows down as LL becomes more saturated with iodine and presumably the iodine adsorbs deeper into the LL particulates. CA, on the other hand, did not absorb iodine readily; gaining only about 2 wt % for the 1 h treatment and about 20 wt % after the 24 h treatment, changing from white to dark yellow. Thus, it is likely that there is only a very weak interaction between CA and iodine as expected by its nonaromatic structure.

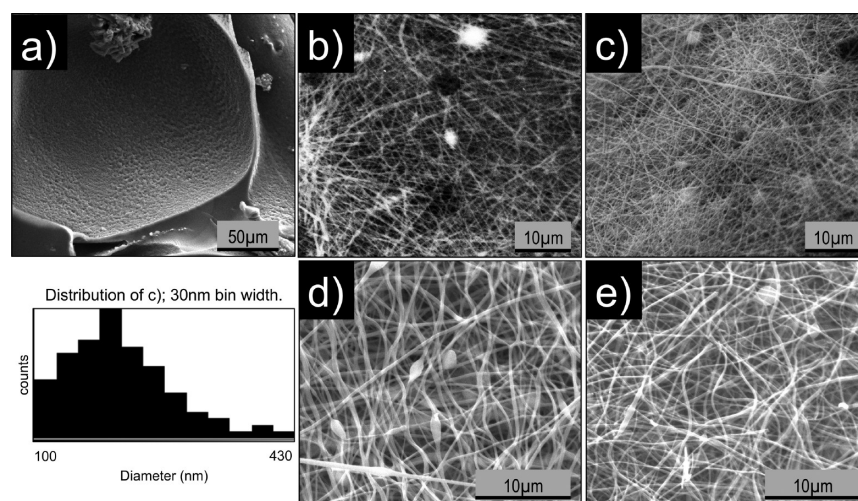


Figure 9. SEM micrographs of the carbonized (1 h in N_2) (a) untreated and thermostabilized (300 °C, 2 h in air) 2:1 ratio LL:CA fibers at 600 °C and the 20 min iodinated and thermostabilized (300 °C, 2 h in air) LL:CA fibers (b) 2:1 ratio at 800 °C, (c) 2:1 ratio at 1000 °C, (d) 4:1 ratio at 800 °C, and (e) 4:1 ratio at 1000 °C. The histogram shows an example diameter distribution as measured for the 2:1 ratio LL:CA fibers carbonized at 1000 °C.

Table 1. Carbon Content (wt %) of As-Spun and Carbonized (carb.) Electrospun Fibers As Measured Using EDS Elemental analysis

LL:CA	as-spun	800 °C carb.	1000 °C carb.
2:1	67.5 ± 0.9	82.5 ± 0.7	94.4 ± 0.5
4:1	69.7 ± 0.7	93.5 ± 0.8	92.8 ± 0.9

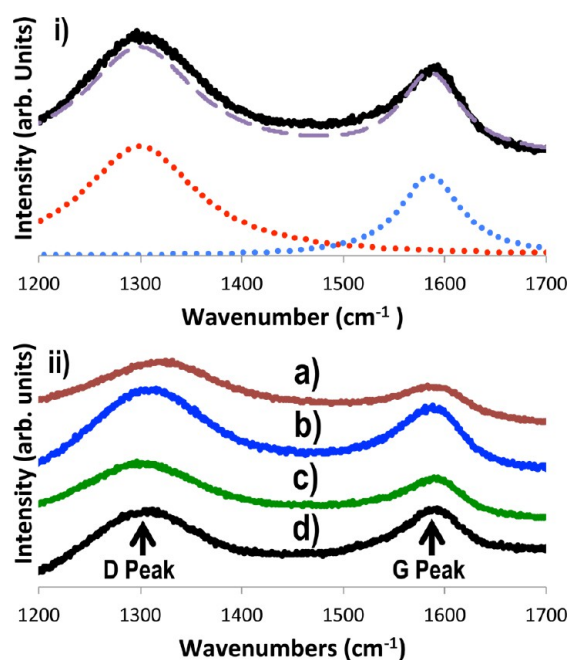


Figure 10. (i) Representative fitted Raman curve of the produced CFs for the 2:1 ratio LL:CA fibers carbonized at 1000 °C. The dotted lines are the fitting curves. The dashed line is the summed fitting curves. The solid line is the measured spectrum. (ii) Representative Raman spectra of LL:CA fibers 20 min iodinated, thermostabilized (300 °C, 2h in air), and carbonized (in N_2): (a) 2:1 ratio at 800 °C, (b) 2:1 ratio at 1000 °C, (c) 4:1 ratio at 800 °C, and (d) 4:1 ratio at 1000 °C.

The thermal degradation mechanisms of the iodine-treated LL and CA samples were investigated through TGA (Figure 3). The TGA thermograms show that neat LL and CA begin to

degrade at 207 and 266 °C, respectively. After iodination, a large degradation beginning at 70 °C is very apparent in LL and small but present in CA. This is attributed to iodine compounds such as HI, CH_3I , C_2H_5I , and I_2 being removed from the polymers.^{26,27} The initial degradation of the iodine-treated LL chains occurs later than neat LL, beginning at 300 °C. The degradation curve of CA iodinated for low time periods did not differ significantly from the curve of the neat CA. However, CA iodine treated for longer time periods (4 h and longer) exhibited a secondary degradation of the CA chains at around 470 °C, which completely degraded the polymer. The yield of the LL samples at 800 °C steadily increases with iodine absorption. The neat LL has a yield at 800 °C, as measured through the TGA, of 36 wt %. After a 1 h iodine treatment, this increased to 44 wt % (normalized to the mass of the lignin before iodine treatment) and by 4 h of iodination increased to 52 wt %. The yields resulting from further iodination times remain relatively constant. Thus, in the treatment of the lignin powders, there seems to be a maximum treatment time to increase the carbonization yield after which there is no additional improvement. The yield of the neat CA was 11 wt %, which did not change after 1 h of iodination, but after 4 h of iodination, the sample was completely degraded at 800 °C. Thus, for CA, iodination does not improve the carbon yield and too much iodination weakens the structure significantly; making it less thermally stable at higher temperatures.

Thermal stabilization was performed on the neat and iodinated LL and CA samples to 300 °C in an air atmosphere at 2 °C/min, holding for 2 h. After heating, the neat brown LL powder fused into a sticky black mass. The iodinated LL powder, however, remained as a black powder. Neat CA did not change at all visually upon heating, but the iodinated CA returned back to a white color, indicating that all the iodine was likely only adsorbed onto the surface of the CA powder.

The thermally stabilized sample powders were then carbonized to 600 °C in an N_2 atmosphere at 2 °C/min holding for 1 h. After this low temperature carbonization, neat iodinated CA and neat LL were all converted into a black macroporous solid mass. However, the iodinated LL remained

Table 2. D and G Peak Parameters, R Value, and Estimated L_a and x_G Values of 2:1 Ratio LL:CA Fibers Carbonized at 800 and 1000 °C and 4:1 Ratio LL:CA Fibers Carbonized at 800 and 1000 °C^a

sample (LL:CA ratio, carb. temp.)	D peak		G peak		R	L_a (nm)	x_G
	position (cm ⁻¹)	fwhm (cm ⁻¹)	position (cm ⁻¹)	fwhm (cm ⁻¹)			
2:1, 800 °C	1318.4	142.7	1584.8	81.6	3.8890	23.434	0.205
2:1, 1000 °C	1300.6	136.9	1584.7	75.6	3.5130	25.942	0.222
4:1, 800 °C	1303.8	139.5	1585.4	76.3	3.5064	25.991	0.222
4:1, 1000 °C	1299.6	136.8	1584.9	71.0	4.1842	21.781	0.193

^aPrior to thermal treatments, the samples were iodine treated for 20 min. Samples were then thermostabilized using a ramp rate of 2 °C/min and holding at 300 °C for 2 h in an air atmosphere. Carbonization was then performed in a N₂ atmosphere using a ramp rate of 2 °C/min and holding at the carbonization temperature (carb. temp.) for 1 h.

a black powder. EDS analysis detected only carbon and oxygen in the samples and measured a carbon content of about 93 and 95 wt % for LL and CA (only measured on surface of samples), respectively, regardless of if they were iodinated or not (carbon contents of neat LL and CA were about 75.0 ± 1.1 and 57.5 ± 1.3 wt %, respectively). Thus, iodination did not affect the resultant carbon content of the carbonized materials. SEM images of the four carbonized samples are shown in Figure 4. As shown, iodinated LL retained its fine powder morphology, while the other three samples became relatively featureless masses. Thus, it is clear that iodine treatment will only have a significant effect on LL in the blend fibers. Thus, it is important for the fibers to contain a high LL content relative to CA in order to take advantage of the effects of the iodine treatment.

From the weight changes, carbon yields, and carbonized morphologies, it is clear that there is an optimal iodination time close to 4 h for the two powders, past which further iodination either does not have a significant effect or is detrimental to the polymer. As expected by their respective structures, there is a much larger interaction between iodine and LL than with CA, and the positive effect of iodination is mainly seen in LL, with higher carbon yields and morphology retention. The iodine does not seem to have a significant effect on the final chemical composition of the carbonized materials.

Effects of Iodine Treatments on Blend Fibers. The electrospun blend fibers were treated with the same iodination process by placing the extracted fibers mats into a ceramic boat. However, it was discovered that past 1 h of iodination, the fiber structure would collapse (Figure 5) and the fiber mat would condense into a hard bead. Figure 5a shows fibers on the verge of collapsing due to iodination where they are swelling, fusing, and breaking. Figure 5b shows a fiber mat after its fiber structure has been completely destroyed due to an extended iodine treatment. A similar effect was observed by Tanabe et al. for coal tar pitches³⁶ in which they found that when the amount of iodine absorbed exceeded a certain threshold of iodine to absorbate molecule, the absorbate melted. This melting was caused by the CTCs acting as permanent dipoles (with the iodine as the anion and aromatic as the cation), which developed electrostatic repulsions strong enough to overcome the energy barrier to viscous flow.³⁶ Thus, there is a limit to how long a sample can be iodinated if morphology retention is desired and thus, the iodination time is even more sensitive in the case of the blend fibers compared to the neat powders.

Although the fibers cannot be iodinated for long time periods, they absorb iodine much faster compared to the neat powders. As expected, the fibers with higher LL contents absorbed more iodine for the same iodination period. After only 15 min of iodine treatment, the 1:1, 2:1, 3:1, and 4:1 ratio LL:CA fibers absorbed 18.5, 37.5, 41.4, and 52.1 wt % of iodine,

respectively. This faster absorption rate is attributed to the high surface area of the fibers compared to the neat powders (~450 nm diameter fibers vs tens of microns for the LL powders and hundreds of microns for the CA powders). It is also expected that the core of the fibers will be well iodinated. Thus, prolonged iodination times are not required for the LL:CA fibers, which allows for faster and cheaper treatments. As occasionally even fibers iodinated for 30 or 40 min were found to collapse, a 20 min iodination time was adopted for all subsequent experiments. The fiber diameters did not change noticeably compared to the as-spun fibers after undergoing the 20 min iodine treatment. Thus, the incorporation of iodine into the fibers does not seem to affect the volume of the fibers nor the interaction between LL and CA within the fibers with the appropriate treatment time.

Thermostabilization and Carbonization of LL:CA Fibers. The 2:1 and 4:1 ratio fibers were chosen to test the thermostabilization and carbonization of the LL:CA fibers due to their low beading levels and high lignin contents. The thermostabilization temperature, ramp rate, and dwell time were set after a series of tests to determine parameters that could produce fibrous CFs after carbonization and TGA results. The fiber mats were wrapped around a wire frame before stabilization as the added tension retains polymer orientation during thermostabilization; a well-known fact from conventionally produced CFs.³⁷ After thermostabilization, the non-iodinated fibers were significantly warped and had some swelling (Figure 6a), while there was no significant change in the fiber morphology or diameter of the iodinated fibers (Figure 6b).

Through EDS elemental analysis, it was determined that all the iodine absorbed into the fibers was removed during the thermostabilization process. FTIR spectra comparing LL:CA fibers as spun, iodinated, thermostabilized, and carbonized are shown in Figure 7 (normalized to a lignin aromatic peak at 1600 cm⁻¹). After iodination and thermostabilization, there was no change in the spectrum of the fibers, showing that no new IR-active bonds were formed during the thermostabilization process. After carbonization, no features were visible in the IR spectra as expected for carbonaceous materials. TGA thermograms of the 2:1 ratio as-spun fibers and the iodinated and thermostabilized fibers are shown in Figure 8. The 2:1 ratio fibers exhibit a single degradation starting at 230 °C and have a yield at 800 °C of 30 wt %; in between the yields of LL and CA. TGA thermograms of the stabilized fibers were similar to that of the neat fibers. They possessed the same initial degradation but they also possessed a small secondary degradation at 725 °C and had a yield at 800 °C of 44 wt %. Thus, the thermostabilization process appeared to change the degradation mechanism of the fibers slightly. The yield of the fibers after the

thermostabilization process was about 90 wt % relative to the as-spun fibers.

The stabilized fibers were then carbonized at 800 and 1000 °C (Figure 9). The fibers that were not iodinated prior to stabilization produced a brittle mat, which did not retain a fibrous morphology, and were degraded into a solid mass (Figure 9a), even at the low carbonization temperature of 600 °C. The iodinated and stabilized fibers, however, retained their fiber structure after carbonization, producing flexible black mats. It was obvious that the fiber mats had shrunk significantly during the carbonization process. The reason for this was clear from the SEM micrographs of the fibers (Figure 9b–e) as the fiber diameters were reduced by about half from ~400–500 nm in the as-spun fibers to ~200–300 nm in the carbonized fibers. As the fiber diameters did not vary significantly between the four carbonized samples, it appears the fibers shrank to a minimum value not influenced by carbonization temperature or precursor fiber composition. The fiber diameter did not vary significantly between the two LL:CA compositions or carbonization temperatures used. The histogram shown in Figure 9 also shows that the normal distribution of the fiber diameters was retained. Carbonization between 1000 and 1200 °C was also attempted but the fibers were either completely degraded or very brittle after carbonization. Thus, higher carbonization temperatures may require further optimization of iodination and stabilization conditions or further treatments.

The carbon wt % values in the carbonized fibers as measured through EDS spectroscopy are shown in Table 1. The 2:1 ratio LL:CA fibers carbonized at 800 °C possessed a lower carbon content compared to the 2:1 ratio LL:CA fibers carbonized at 1000 °C. The 4:1 ratio carbonized at both temperatures contained a similar carbon content; which was close to the carbon content of the carbonized LL and CA powders. Thus, there seems to be a limit to the level of carbonization obtainable for these LL:CA materials of about 94 wt % carbon. As the 4:1 ratio fibers reached this carbonization level at 800 °C while the 2:1 fibers did not, CA may hinder the carbonization process. Thus, for iodination, carbonization, and utilization of lignin, it is highly desirable to reduce the CA content in the fibers as much as possible while maintaining its spinability and morphology.

Raman Spectroscopy of Carbonized LL:CA Fibers.

Raman spectroscopy is an important tool for the characterization of carbonaceous materials. Two main peaks are used to characterize the degree in which the carbon atoms in the carbonaceous material are bonded with sp^3 “disordered” bonds (D peak centered around 1360 cm^{-1}) and the more highly ordered in-plane sp^2 “graphitic” bonds (G peak centered around 1580 cm^{-1}).³⁸ The $R = I(D)/I(G)$ ratio is the ratio of the integrated areas below the D and G peaks integrated between the limits of their full width at half-maximum (fwhm). The value of this ratio depends on both the alignment of the graphitic planes in the sample and degree of graphitization; with lower values representing more sp^2 carbons.³⁸ R can also be used to determine the in-plane graphitic crystallite size L_a and the graphitic mole fraction x_G . Cancado et al.³⁹ developed a general equation for finding the L_a through Raman spectroscopy using the R value and laser line wavelength (λ_L) in nanometers

$$L_a \text{ (nm)} = (2.4 \times 10^{-10}) \lambda_L^4 / R \quad (1)$$

x_G can also be calculated to a first order approximation by

$$x_G = \frac{I(G)}{I(D) + I(G)} = \frac{1}{1 + R} \quad (2)$$

by assuming that $I(D)$ and $I(G)$ have the same proportional coefficient.⁴⁰ Representative Raman spectra of the prepared CFs and examples of the fitting curves used to isolate the D and G peaks are shown in Figure 10. Table 2 shows the peak position and fwhm of the D and G peaks as well as the calculated R , L_a , and x_G values. The D peaks were centered around 1300 cm^{-1} , which is on the extreme end of where D peaks can be located⁴¹ and is significantly shifted from the typical position of D peaks in PAN-based electrospun CFs between 1350 and 1380 cm^{-1} .^{38,40,42} The R and x_G values are larger than that of most PAN-based CFs,⁴⁰ indicating lower levels of graphitization. While in the 2:1 ratio fibers, the level of graphitization increased with carbonization temperature, as is typical, in the 4:1 ratio fibers, it decreased. Thus, it seems that the higher LL content acts to promote more disordered type carbon bonds likely due to the amorphous nature of lignin compared to CA, which would be expected to exhibit more molecular orientation. Compared to PAN-based CFs,⁴⁰ the lignin-based CFs had much larger L_a values. Thus, it appears that while there is less graphitization in the LL:CA blend fibers, the in-plane graphitic crystallites that do form are much larger than in PAN-based CFs.

CONCLUSION

Pure biopolymer-composed precursor-based carbon fibers were successfully electrospun from blends of organosolv lignin and cellulose acetate up to a lignin:cellulose acetate ratio of 4:1. The lignin and cellulose acetate exhibited an excellent interaction that allowed fibers to be fabricated from concentrations that would not be possible for pure polymers. Iodine treatments were investigated for their influence on the carbonization behavior of lignin and cellulose acetate and their electrospun blend fibers. The iodine treatments were found to significantly enhance the morphology retention of lignin and the blend fibers due to the selective interaction of the iodine. The blend fibers were successfully converted into carbon fibers using carbonization temperatures of up to 1000 °C. Raman analysis confirmed that the carbonization temperature significantly influenced the graphitization of the LL:CA fibers. The final carbonized fibers shrank to ~250 nm in diameter. Compared to CFs produced from polyacrylonitrile, the CFs produced from the LL:CA fibers had less overall graphitization but formed larger in-plane graphitic crystals. Overall, the produced lignin–cellulose acetate fibers and their iodine treatment show significant promise toward improving the production of cheap and green carbon fibers in a quick and efficient manner.

AUTHOR INFORMATION

Corresponding Author

*E-mail: mmisra@uoguelph.ca. Tel: 519-824-4120, ext. 58935, 56766. Fax: 519-836-0227.

Present Address

S. Vivekanandhan: Department of Physics, VHNSN College, Virudhunagar, 626001, Tamilnadu, India.

Notes

The authors declare no competing financial interest.

ACKNOWLEDGMENTS

This research is financially supported by the Natural Sciences and Engineering Research Council (NSERC), Canada, for the Discovery grant to M. Misra (NSERC-NCE AUTO21); the Ontario Research Fund, Research Excellence, Round-4 (ORF RE04) from the Ontario Ministry of Economic Development and Innovation (MEDI); the Ontario Ministry of Agriculture Food and Rural Affairs (OMARA)- New Directions & Alternative Renewable Fuels Research program; and OMA-FRA- University of Guelph Bioeconomy-Industrial uses Research Program. The authors are also thankful to Lignol Innovations, Ltd., Burnaby, BC, Canada, for providing the organosolv lignin samples and advice.

REFERENCES

- (1) Chand, S. Carbon fibres for composites. *J. Mater. Sci.* **2000**, *35*, 1303–1313.
- (2) Huang, X. Fabrication and properties of carbon fibers. *Materials* **2009**, *2*, 2369–2403.
- (3) MacDiarmid, A. G.; Jones, W. E.; Norris, I. D.; Gao, J.; Johnson, A. T.; Pinto, N. J.; Hone, J.; Han, B.; Ko, F. K.; Okuzaki, H.; Llaguno, M. Electrostatically-generated nanofibers of electronic polymers. *Synth. Met.* **2001**, *119*, 27–30.
- (4) Inagaki, M.; Yang, Y.; Kang, F. Carbon nanofibers prepared via electrospinning. *Adv. Mater.* **2012**, *24*, 2547–2566.
- (5) Kim, C.; Ngoc, B. T. N.; Yun, W. Y.; Lee, J.-W.; Yang, K. S. Fabrications and Electrochemical Properties of Two-Phase Activated Carbon Nanofibers from Electrospinning; Nanotechnology Materials and Devices Conference, IEEE, Gyeongju, South Korea, October 22–25, 2006.
- (6) Park, S. H.; Kim, C.; Jeong, Y. I.; Lim, D. Y.; Lee, Y. E.; Yang, K. S. Activation behaviors of isotropic pitch-based carbon fibers from electrospinning and meltspinning. *Synth. Met.* **2004**, *146*, 207–212.
- (7) Edie, D. D. The effect of processing on the structure and properties of carbon fibers. *Carbon* **1998**, *36* (4), 345–362.
- (8) Reneker, D. H.; Chun, I. Nanometre diameter fibres of polymer, produced by electrospinning. *Nanotechnology* **1996**, *7*, 216–223.
- (9) Kakade, M. V.; Givens, S.; Gardner, K.; Lee, K. H.; Chase, D. B.; Rabolt, J. F. Electric field induced orientation of polymer chains in macroscopically aligned electrospun polymer nanofibers. *J. Am. Chem. Soc.* **2007**, *129*, 2777–2782.
- (10) Bacon, R.; Tang, M. M. Carbonization of cellulose fibers—II. Physical property study. *Carbon* **1964**, *2*, 221–225.
- (11) Singer, L. S. Carbon fibres from mesophase pitch. *Fuel* **1981**, *60*, 839–847.
- (12) Seydibeyoğlu, M. Ö. A novel partially biobased PAN-lignin blend as a potential carbon fiber precursor. *J. Biomed. Biotechnol.* **2012**, *2012*, 1–8.
- (13) Kadla, J.; Kubo, S.; Venditti, R.; Gilbert, R.; Compere, A.; Griffith, W. Lignin-based carbon fibers for composite fiber applications. *Carbon* **2002**, *40*, 2913–2920.
- (14) Sudo, K.; Shimizu, K. A new carbon fiber from lignin. *J. Appl. Polym. Sci.* **1992**, *44*, 127–134.
- (15) Kubo, S.; Uraki, Y.; Sano, Y. Preparation of carbon fibers from softwood lignin by atmospheric acetic acid pulping. *Carbon* **1998**, *36*, 1119–1124.
- (16) Poursorkhabi, V.; Misra, M.; Mohanty, A. K. Extraction of lignin from a coproduct of the cellulosic ethanol industry and its thermal characterization. *BioResources* **2013**, *8*, 5083–5101.
- (17) Poursorkhabi, V.; Mohanty, A. K.; Misra, M. Electrospinning of aqueous lignin/poly(ethylene oxide) complexes. *J. Appl. Polym. Sci.* **2014**, DOI: 10.1002/app.41260.
- (18) Kumar, S.; Mohanty, A. K.; Erickson, L.; Misra, M. Lignin and its applications with polymers. *J. Biobased Mater. Bioenergy* **2009**, *3*, 1–24.
- (19) Choi, D. I.; Lee, J.-N.; Song, J.; Kang, P. H.; Park, J.-K.; Lee, Y. M. Fabrication of polyacrylonitrile/lignin-based carbon nanofibers for high-power lithium ion battery anodes. *J. Solid State Electrochem.* **2013**, *17*, 2471–2475.
- (20) Kadla, J. F.; Kubo, S. Lignin-based polymer blends: analysis of intermolecular interactions in lignin–synthetic polymer blends. *Composites, Part A* **2004**, *35*, 395–400.
- (21) Seo, D. K.; Jeun, J. P.; Bin Kim, H.; Kang, P. H. Preparation and characterization of the carbon nanofiber mat produced from electrospun PAN/lignin precursors by electron beam irradiation. *Rev. Adv. Mater. Sci.* **2011**, *28*, 31–34.
- (22) Chatterjee, S.; Jones, E. B.; Clingenpeel, A. C.; McKenna, A. M.; Rios, O.; McNutt, N. W.; Keffer, D. J.; Johs, A. Conversion of lignin precursors to carbon fibers with nanoscale graphitic domains. *ACS Sustainable Chem. Eng.* **2014**, *2*, 2002–2010.
- (23) Schreiber, M.; Vivekanandhan, S.; Cooke, P.; Mohanty, A. K.; Misra, M. Electrospun green fibres from lignin and chitosan: A novel polycomplexation process for the production of lignin-based fibres. *J. Mater. Sci.* **2014**, *49*, 7949–7958.
- (24) Khan, M. M. R.; Gotoh, Y.; Morikawa, H.; Miura, M. Graphitization behavior of iodine-treated *Bombyx mori* silk fibroin fiber. *J. Mater. Sci.* **2009**, *44*, 4235–4240.
- (25) Miyajima, N.; Akatsu, T.; Ito, O.; Sakurovs, R.; Shimizu, S.; Sakai, M.; Tanabe, Y.; Yasuda, E. The rheological behavior during carbonization of iodine-treated coal tar pitch. *Carbon* **2001**, *39*, 647–653.
- (26) Miyajima, N.; Dohi, S.; Akatsu, T.; Yamamoto, T.; Yasuda, E.; Tanabe, Y. Stabilization and carbonization behavior of pitch-model compounds treated with iodine or bromine. *Carbon* **2002**, *40*, 1533–1539.
- (27) Kajiura, H.; Tanabe, Y.; Yasuda, E. Carbonization and graphitization behavior of iodine-treated coal tar pitch. *Carbon* **1997**, *35*, 169–174.
- (28) Khan, R.; Gotoh, Y.; Morikawa, H.; Miura, M. Influence of iodine treatment on the carbonization behavior of *Antheraea pernyi* silk fibroin fiber. *J. Appl. Polym. Sci.* **2008**, *110*, 1358–1365.
- (29) Khan, M. M. R.; Gotoh, Y.; Morikawa, H.; Miura, M.; Fujimori, Y.; Nagura, M. Carbon fiber from natural biopolymer *Bombyx mori* silk fibroin with iodine treatment. *Carbon* **2007**, *45*, 1035–1042.
- (30) Moulay, S. Molecular iodine/polymer complexes. *J. Polym. Eng.* **2013**, *33*, 389–443.
- (31) Miyajima, N.; Yasuda, E.; Rand, B.; Akatsu, T.; Kameshima, K.; Tanabe, Y. Comparison of Bromine-treatment and Iodine-treatment in the carbonization of pitches. *TANSO* **2000**, *2000*, 405–409.
- (32) Schreiber, M.; Vivekanandhan, S.; Mohanty, A. K.; Misra, M. A study on the electrospinning behaviour and nanofiber morphology of anionically charged lignin. *Adv. Mater. Lett.* **2012**, *3*, 476–480.
- (33) Glasser, W. G.; Rials, T. G.; Kelly, S. S.; Davé, V. Studies of the Molecular Interaction between Cellulose and Lignin as a Model for the Hierarchical Structure of Wood. In *Cellulose Derivatives: Modification, Characterization, and Nanostructures*; Heinze, T. J., Glaser, W. G., Eds.; ACS Symposium Series 688; American Chemical Society: Washington, DC, 1998; pp 265–282.
- (34) Davé, V.; Glasser, W. G. Cellulose-based fibres from liquid crystalline solutions: 5. Processing and morphology of CAB blends with lignin. *Polymer* **1997**, *38*, 2121–2126.
- (35) Goring, D. The physical chemistry of lignin. *Pure Appl. Chem.* **1962**, *5*, 233–54.
- (36) Tanabe, Y.; Tanaka, F.; Takahashi, M.; Iiyama, T.; Miyajima, N.; Fujisawa, S.; Yasuda, E. Sorption behavior of iodine vapor into pitches and its stabilizing mechanism below the melting temperature of the pitches. *Carbon* **2004**, *42*, 1555–1564.
- (37) Wu, G.; Lu, C.; Ling, L.; Hao, A.; He, F. Influence of tension on the oxidative stabilization process of polyacrylonitrile fibers. *J. Appl. Polym. Sci.* **2005**, *96*, 1029–1034.
- (38) Kim, C.; Park, S. H.; Cho, J.-I.; Lee, D.-Y.; Park, T.-J.; Lee, W.-J.; Y, K.-S. Raman spectroscopic evaluation of polyacrylonitrile-based carbon nanofibers prepared by electrospinning. *J. Raman Spectrosc.* **2004**, *35*, 928–933.
- (39) Cancado, L. G.; Takai, K.; Enoki, T.; Endo, M.; Kim, Y. A.; Mizusaki, H.; Jorio, A.; Coelho, L. N.; Magalhaes-Paniago, R.; Pimenta,

M. A. General equation for the determination of the crystallite size L_a of nanographite by Raman spectroscopy. *Appl. Phys. Lett.* **2006**, *88*, 163106–163106–3.

(40) Wang, Y.; Serrano, S.; Santiago-Avilés, J. J. Raman characterization of carbon nanofibers prepared using electrospinning. *Synth. Met.* **2003**, *138*, 423–427.

(41) Schwan, J.; Ulrich, S.; Batori, V.; Ehrhardt, H.; Silva, S. R. P. Raman spectroscopy on amorphous carbon films. *J. Appl. Phys.* **1996**, *80*, 440–447.

(42) Zussman, E.; Chen, X.; Ding, W.; Calabri, L.; Dikin, D. A.; Quintana, J. P.; Ruoff, R. S. Mechanical and structural characterization of electrospun PAN-derived carbon nanofibers. *Carbon* **2005**, *43*, 2175–2185.